

**Determination of the Failure Susceptibility of a Flat Die used
in Biomass Pelletizing Machines by means of FEA based
Design Exploration**

Journal:	<i>Journal of Failure Analysis and Prevention</i>
Manuscript ID	Draft
Manuscript Type:	Technical Article
Date Submitted by the Author:	n/a
Complete List of Authors:	Celik, H.Kursat; Akdeniz Universitesi, Dept. of Agricultural Machinery and Technology Engineering; Lancaster University, Lancaster Product Development Unit Yilmaz, Hasan; Akdeniz University, Dept. of Agricultural Machinery and Technology Engineering Rennie, Allan E. W.; Lancaster University, Lancaster Product Development Unit Cinar, Recep; Yenasoft Ltd., 3Engineering Bureau Firat, M. Ziya; Akdeniz University, Dept. of Animal Science
Keywords:	Stress analysis, Design of agricultural machinery, Biomass pelletizing, flat die design

SCHOLARONE™
Manuscripts

Determination of the Failure Susceptibility of a Flat Die used in Biomass Pelletizing Machines by means of FEA based Design Exploration

H. Kursat Celik^{1*}, Hasan Yilmaz¹, Allan E.W. Rennie², Recep Cinar³, M. Ziya Firat⁴

¹Department of Agricultural Machinery and Technology Engineering, Faculty of Agriculture, Akdeniz University, Antalya, Turkey

²Lancaster Product Development Unit, Engineering Department, Lancaster University, Lancaster, United Kingdom

³Engineering Bureau, Yenasoft Inc., Istanbul, Turkey

⁴Department of Animal Science, Faculty of Agriculture, Akdeniz University, Antalya, Turkey

Correspondence	: Dr H. Kursat CELIK
e-mail	: hkcelik@akdeniz.edu.tr
Tel	: +90 242 310 65 70
Fax	: +90 242 227 45 64
Address	: Department of Agricultural Machinery & Tech. Engineering, Faculty of Agriculture, Akdeniz University, 07070, Antalya, Turkey

Abstract

This paper focuses on a design analysis of a flat die used in an agricultural biomass pelletizing machine by considering its high pressure loading failure susceptibility. The pellet die is one of the key elements in a pelletizing machine, and the strength of the die plate has an important role on the pellet's quality and producibility. In fact, higher compression ratio (CR - the ratio of effective length and the internal (press channel) diameter of a die orifice/hole) will provide denser pellets which is a desired phenomenon, however, if the compression pressure is too high or CR is not determined to compensate high pressures, the raw material may block the die and the die may experience deformation failure due to overloading. If the desire is to make high quality pellets with no die failure, optimum flat die hole/orifice design parameters should be used which can provide the best CR for a specific compression pressure. This is the core motivation of this research. In this study, Finite Element Analysis (FEA) based design exploration has been utilised for a sample single hole flat die with various die geometry parameters against various compression pressure values. Following the FEA design exploration undertaken, a response surface analysis (RSA) was carried out and then estimation models (empirical equations), which could be used to calculate parameters of the die hole/orifice against applied compression pressure and failure susceptibility based on structural stress and deformation, was described. The results gained from the RSA has indicated that the estimation models have high R^2 values (higher than 98 %) which could be used for adequately predicting failure susceptibility indicators. In addition to this, FEM-based simulation print-outs have provided useful stress distribution visuals on the die against different compression pressure values. Most especially, the study has highlighted that a detailed structural optimisation study may be scheduled in order to obtain die geometry design parameters with a focus on the failure susceptibility.

Keywords: Stress analysis, design of agricultural machinery, biomass pelletizing, flat die design.

1. Introduction

Biomass pellets are one of the alternative solid fuels which are usually made from agricultural and forestry residues. The main advantages of pelletisation are efficient combustion in automatic combustion systems, higher energy efficiency, and higher bulk density with uniform geometric shape which can facilitate handling/packaging operations for loading and transportation etc.

(Werther *et al.*, 2000; Mani *et al.*, 2003; Holm *et al.*, 2006; Nilsson *et al.*, 2011; Theerarattananon *et al.*, 2011; Garcia-Maraver *et al.*, 2011; Celma *et al.*, 2012; Zamorano *et al.*, 2011).

In the pellet production, which can be described as in **Figure 1**, reducing the cost of pelletizing operations with high quality pellet production is the key desire/target. To address this target, although feedstock type and its specifications such as moisture content, particle size, compression pressure etc. are important, having a well-designed pellet die (as the main functional machine element of pelletizing systems) plays a significant role.

(**Figure 1**. Biomass pelletizing process)

The literature describes a number of biomass pelletizing processes with various feedstock types, particle sizes, moisture contents, compression pressures and pelletizers with various die designs, however, it would not be wrong to say that research related to the design of an optimum die by means of computer aided engineering and structural optimisation approaches is very limited (Jackson *et al.*, 2016; CPM 2015; Puig-Arnabat *et al.*, 2016. Yilmaz 2014; Ciolkosz *et al.*, 2015; Stelte *et al.*, 2011; Salas-Bringas *et al.*, 2010; Hu *et al.*, 2012; Mani *et al.*, 2004; Döring 2013; Holm *et al.*, 2006, Peng J. H. *et al.*, 2013).

The literature highlights that each kind of feedstock has its own characteristics. These characteristics and the pelletizing conditions are important in terms of selecting the correct pelletizing machine and its functional elements/components such as the die. One specific feature of

1 a die structure used in a pelletizing machine, which can fundamentally affect the pelletizing process
2
3 and resultant pellet quality, is the compression ratio (CR) which is defined as the ratio of the
4
5 effective length and the internal diameter of a die orifice/hole. The CR of pellet mill dies is
6
7 determined by consideration of raw biomass materials. For example, the best CR for sawdust is
8
9 reported as 4.5:1, however, different materials may have different (smaller or larger) CRs
10
11 (ABC Machinery 2017a, 2017b; Moon *et al* 2014). If the CR of pellet mill dies is not suitable,
12
13 production losses can be experienced. Therefore, selection of the die with appropriate geometric
14
15 specifications for a successful pelletizing operation of the desired raw materials is an important
16
17 issue to be considered in the design of the pellet mills and its functional components.
18
19

20
21 Pellet mills can be classified according to types of die. Basically, they can be divided into two
22
23 types: flat and ring dies. The structure of a flat pellet die can be simply described as a solid metal
24
25 plate with holes/orifices sitting below a series of compression rollers. Material enters from above
26
27 and falls between the rollers, which is then compressed through the die. Flat die pellet mills are
28
29 used in small-to-medium or farm scale pellet industries and they are featured for easy to maintain,
30
31 low capacity and are cheaper than the ring die. The ring die pellet mills are used for large scale and
32
33 commercial pellet industries. These types of dies can have additional advantages such as high
34
35 production capacity, less mechanical wear, a relatively durable structure and they can enable low
36
37 energy consumption, however, large scale production investigation is essential in their usage
38
39 (Garcia-Maraver and Carpio 2015; PelHeat 2015; Protić *et al* 2011). Although flat die pellet mills
40
41 have some disadvantages relative to ring die pellet mills (in terms of pelleting capacity), it is a very
42
43 appropriate type of die in order to maintain adequate production for small scale farm producers.
44
45

46
47 For structural strength, the die is also the key element in a pelletizing machine. The major reason
48
49 for this is that a great deal of force is exerted on the raw material as it progresses through the pellet
50
51 production process in order to move them into the holes at the die. This pressure should be
52
53 compensated by the die geometry for minimum energy consumption and high quality denser pellet
54
55
56
57
58
59
60

1 production, which are essential requirements in this process (Garcia-Maraver and Carpio 2015;
2 Stelte *et al.* 2011).
3
4

5
6 In the pelletizing process, if the compression pressure is too high or CR is not determined to
7 compensate for high pressures, the raw material may block the die and the required high
8 compression pressure may rise. This may cause undesired machine failures because of overloading
9 such as wear and abrasion inside the die orifices, cracks or plastic deformation on the pellet die.
10 These types of failures cause production losses or undesired pellet shapes and high levels of energy
11 consumption. In this context, some failure samples seen on the die elements are shown in Figure 2.
12 In addition to mechanical failures caused by high pressure, high temperature based die failures can
13 also be seen on the die elements as while the particles are passing through the die, frictional heating
14 occurs during pelletizing. The increase in particle size would explain the higher temperature rise
15 caused by greater frictional heating in the die (Briggs *et al.* 1999).
16
17
18
19
20
21
22
23
24
25
26
27
28
29

30 (Figure 2. Some failure samples seen on the die element)
31
32
33

34 This failure phenomenon on the dies push us to seek solutions for prevention from these
35 undesired die failures. In this manner, the determination of optimum flat die hole/orifice design
36 parameters can provide the best CR for a specific compression pressure for producing a high quality
37 pellet and it may provide less risk for potential die failures. This is the core motivation for the
38 research detailed in this paper. This study introduces a Finite Element Analysis (FEA) based design
39 exploration for sample single hole flat die design parameters (geometry dimensions) against various
40 compression pressure values. Numerical outputs from FEA based exploration have been utilised for
41 response surface analysis (RSA). Subsequently, estimation models (empirical equations) which may
42 be used to calculate parameters of the die hole/orifice against applied compression pressure and
43 failure susceptibility based on structural/mechanical stress and deformation, was described through
44 RSA data.
45
46
47
48
49
50
51
52
53
54
55
56
57
58
59
60

2. 3D Solid Modelling and Finite Element Analysis

The FEA was set up in order to simulate deformation behaviour and distribution of the equivalent stress areas on the flat die hole surfaces during pelleting compression. Different flat die moulds with specific die orifice designs are needed for different types of pellets and different raw material processing. Holm *et al.* (2006) suggested a pellet die design with 6 [mm] outlet orifice diameter and obtained pellets approximately 6 [mm] diameter and 18 [mm] in length. Other related literature and standards also make suggestions for pellet diameter in the ranges of 6 [mm] to 8 [mm] (Jackson *et al* 2016; Milovančević *et al* 2010; Zamorano *et al* 2011; EN 16127:2013). In consideration of the literature, at the initial stage, appropriate dimensions have been appointed for the die hole considering the pelletizing loading conditions with effective pellet diameter of 6 [mm] (Figure 3). Solid models used in the FEA of the single hole die were modelled in SolidWorks parametric 3D-solid modelling software. ANSYS Workbench commercial FEA code was utilised for the simulation of the loading scenario. Homogeneous isotropic linear elastic material model and linear static loading condition assumptions were considered in the FEA setup. Material properties for stainless steel (ANSYS Workbench Material Library) were appointed for the die model. Compression pressure of 50 [MPa] was applied to the inner surfaces of the die hole for the initial design analysis. It is assumed that the compression pressure uniformly affects the die hole surfaces. The outer circular surface of the die was restricted with fixed support boundary conditions in the FEA code. ANSYS Workbench meshing functions were used to create the FE model of the die. After all pre-processing procedures, the FEA simulation was run, and the results were recorded. The failure threshold in the design analysis simulations has been defined to the plastic deformation point where the equivalent stress value runs beyond the material yield point (210 [MPa]). FEA setup for boundary conditions, mesh structure and simulation print outs for stress and deformation distributions are shown in Figure 3.

(Figure 3. FEA simulation setup, FE model and simulation print outs)

3. Design Exploration

The results gained from the FEA of the initial design analysis setup showed that there were no indications of failure. The maximum Von-Mises equivalent stresses on the die hole surfaces were calculated as 88.445 [MPa] whilst the maximum deformation was 0.0012 [mm] against the initial compression pressure of 50 [MPa]. None of the stresses and/or deformation had a value which could affect the pellet production in any negative manner, however, in order to understand the effect of the different design parameters on the stress/deformation distribution, the sample die was also analysed by means of a RSA approach. This approach was utilised to predict the failure susceptibility and change/effect of the CR for different compression pressures which was not considered in the initial FEA simulation setup. Response surface methodology (RSM) is used for empirical model building. RSM can be described as a collection of mathematical and statistical techniques. Originally, RSM was developed to model experimental responses and then migrated to the modelling of numerical experiments (Box and Draper 1987). In order to obtain the response surfaces, ANSYS Workbench Design Exploration module was utilised and Design of Experiment (DOE) points were setup. DOE is a technique used to determine the location of sampling points and is included as part of the response surface, goal driven optimisation, and six sigma analysis systems, and the main purpose of design exploration is to identify the relationship between the performance of the product (maximum stress, mass, fluid flow, velocities, etc.) and the design variables (dimensions, loads, material properties, etc.) (ANSYS Product, 2017). Initial design parameter setup, constraints and response parameters are given in Table 1. In consideration of the definitions given in Table 1, 25 DOE points in total have been solved by the simulation tool and the resultant data processed. The comparison chart given in Figure 4 is a representation of the comparison of the predictions from solved specific design points and predictions from response surface data. This chart indicates that response surface data predictions are well fitted to the solved specific design

points. Processed data was also converted to response surface charts so that variations of the design parameters against response parameters can be seen. The charts (contour plots) are given in **Figure 5**.

(**Table 1**. Design parameters and response parameters)

(**Figure 4**. Comparison of the predictions from solved specific design points and predictions from response surface data)

(**Figure 5**. Response surface charts)

In addition to the chart representations, statistical evaluation of the response surface data in order to predict the failure susceptibility indications such as stress (P5) and deformation (P6) values against various die hole diameter parameters, which are not considered in the initial FEM based simulation set up, has been conducted and the parameters have been estimated. The estimation is expressed by a model described in **Equation 1**.

$$Y_i = \beta_0 + \beta_1 x_{1i} + \beta_2 x_{2i} + \beta_3 x_{1i}^2 + \beta_4 x_{2i}^2 + \beta_5 x_{1i} x_{2i} + \varepsilon_i \quad (1)$$

Here, Y_i is failure susceptibility indication (stress (P5) [MPa] or deformation (P6) [mm]); x_{1i} is first estimation model component; x_{2i} is second estimation model component; β_0 is the intercept; β_1 , β_2 , β_3 , β_4 , and β_5 are the interaction coefficients of linear, quadratic and second order terms, respectively; and ε_i is the error term. The closeness of the fit of the model in **Equation 1** has been evaluated using the coefficient of determination (R^2). The parameter estimates of the model described in **Equation 1** are listed in **Table 2**. According to the RSA results gained, it appears that the estimation models have high R^2 values (higher than 98 %) which can be used for predicting

accurate failure susceptibility indicators. For these twelve models given in [Table 2](#), both variable x_{1i} and x_{2i} and their interaction seem to be very important parameters (see partial F-test and F-test for overall [total] regression results given in [Table 2](#)).

([Table 2](#). Estimation model parameters by RSM charts)

4. Discussion

Initial FEA (for die hole diameter: 6 [mm]; hole length: 18 [mm]; compression pressure: 50 [MPa]) revealed resultant data with no failure track on the die. The safe working coefficient (safety factor) was approximately 2.4 (material yield point equivalent stress reference: see [Figure 3](#)). This showed that the die functions safely under defined initial boundary conditions. Further, the output data has also been successfully used for design exploration which is set up to identify the relationship between the failure susceptibility indications (maximum equivalent stress, maximum deformation) and the die design variables (die hole dimensions and compression pressure). Successful identification of the relationship has been described through RSA. Comparison of the solved specific design points in FEA and predictions from response surface data revealed a good accordance (over 98 % correlation), which could be considered as prediction validation. In this way, useful empirical models (equations) to predict failure susceptibility indicators have been presented through the data obtained from response surface charts.

Failure susceptibility indicators (maximum eq. stress, maximum deformation) have been predicted through empirical models extracted from 12 RSA charts in total. The charts revealed that P1 (effective hole length) is not effective on P5 (the eq. stress) (relative to P2), however, increase in P2 (effective (outlet) hole radius) provide nearly linear decrease in P5 (Chart No: 1). This is because of an increase in surface area where it is exposed to the compression pressure. Increase in P3 (inlet hole radius) and P4 (compression pressure) values provide increase in P5 (Chart No: 3, 5, 7, 9, 11). In a similar approach, P1 is effective on P6 (die hole deformation) and

1 it can be said that an increase in P1 provides an increase in P6. Likewise, an increase in P3 and P4
2 provides an increase in P6, however P2 is not seen as effective on P6 (Chart No: 2, 4, 6, 8, 10, 12).
3

4
5 Estimation model parameters have been extracted from RSM charts which are presented in
6 **Table 2** and revealed high correlation ratios (over 98 %). This shows that the estimation models are
7 quite reliable in predicting failure susceptibility indicators. In the evaluation of CR through the RSA
8 charts, Chart no: 1 and Chart no: 2 show the CR variations (P1 and P2) against failure susceptibility
9 indicators (P5 and P6). The estimation models extracted from Chart no 1 and Chart no 2 can be
10 used precisely for predicting failure susceptibility indicators (P5 and P6) and optimum CR values
11 within the safety range can be calculated. Here, it should be highlighted that the charts related to CR
12 parameters given in **Figure 5** were presented with constant compression pressure and inlet die
13 hole/orifice values. Related charts can be updated within the analysis code for various constant
14 compression pressure and inlet die hole/orifice values in order to explore the change of CR
15 parameters. This is one of the advantages of the computer aided design exploration approach based
16 on FEA.
17
18
19
20
21
22
23
24
25
26
27
28
29
30

31 FEA (for die hole diameter: 6 [mm]; hole length: 18 [mm]; compression pressure: 50 [MPa])
32 revealed resultant data with no failure track on the die. The safe working coefficient (safety factor)
33 was approximately 2.4 (material yield point equivalent stress reference: see **Figure 3**). This showed
34 that the die functions safely under defined initial boundary conditions. Further, the output data has
35 also been successfully used for design exploration which is set up to identify the relationship
36 between the failure susceptibility indications (maximum equivalent stress, maximum deformation)
37 and the die design variables (die hole dimensions and compression pressure). Successful
38 identification of the relationship has been described through RSA. Comparison of the solved
39 specific design points in FEA and predictions from response surface data revealed a good
40 accordance (over 98 % correlation), which could be considered as prediction validation. In this way,
41 useful empirical models (equations) to predict failure susceptibility indicators have been presented
42 through the data obtained from response surface charts.
43
44
45
46
47
48
49
50
51
52
53
54
55
56
57
58
59
60

1 Failure susceptibility indicators (maximum eq. stress, maximum deformation) have been
2 predicted through empirical models extracted from 12 RSA charts in total. The charts revealed that
3
4 P1 (effective hole length) is not effective on P5 (the eq. stress) (relative to P2), however, increase in
5
6 P2 (effective (outlet) hole radius) provide nearly linear decrease in P5 (Chart No: 1). This is
7
8 because of an increase in surface area where it is exposed to the compression pressure. Increase in
9
10 P3 (inlet hole radius) and P4 (compression pressure) values provide increase in
11
12 P5 (Chart No: 3, 5, 7, 9, 11). In a similar approach, P1 is effective on P6 (die hole deformation) and
13
14 it can be said that an increase in P1 provides an increase in P6. Likewise, an increase in P3 and P4
15
16 provides an increase in P6, however P2 is not seen as effective on P6 (Chart No: 2, 4, 6, 8, 10, 12).
17
18
19
20

21 Estimation model parameters have been extracted from RSM charts which are presented in
22
23 **Table 2** and revealed high correlation ratios (over 98 %). This shows that the estimation models are
24
25 quite reliable in predicting failure susceptibility indicators. In the evaluation of CR through the RSA
26
27 charts, Chart no: 1 and Chart no: 2 show the CR variations (P1 and P2) against failure susceptibility
28
29 indicators (P5 and P6). The estimation models extracted from Chart no: 1 and Chart no: 2 can be
30
31 used precisely for predicting failure susceptibility indicators (P5 and P6) and optimum CR values
32
33 within the safety range can be calculated. Here, it should be highlighted that the charts related to CR
34
35 parameters given in **Figure 5** were presented with constant compression pressure and inlet die
36
37 hole/orifice values. Related charts can be updated within the analysis code for various constant
38
39 compression pressure and inlet die hole/orifice values in order to explore the change of CR
40
41 parameters. This is one of the advantages of the computer aided design exploration approach based
42
43 on FEA.
44
45
46
47
48

49 **5. Conclusions**

50
51 Details of the study have introduced a FEA based design exploration methodology for prediction
52
53 of failure susceptibility indicators by considering CR parameters of a flat die under defined
54
55 boundary conditions. FEA based design exploration and RSA have proved useful in numerical and
56
57
58
59
60

1 visual evaluation contexts. A failure evaluation was carried out considering the failure criterion
2 (yield point) of the die materials and failure susceptibility indicators: Eq. stress and deformation.
3
4 The indicator values were calculated through estimation models extracted from a FEA aided design
5
6 explorer study.
7
8

9
10 The FEM based analysis can help in reducing turn-around time, automating the total design
11 analysis process by eliminating manual operations. Additionally, the FEA approach can be used
12 efficiently for similar pelletizing machinery elements used in agricultural machinery systems.
13
14 However, validation is an important process in order to evaluate the accuracy of FEM based
15 simulations against the physical test and/or analytical results. Therefore, for future research agenda,
16 experimental validation through experimental stress analysis of this work should be considered.
17
18 Physical validation of the empirical equation against FEA and RSA exploration is a significant
19 requirement. Another point to be considered in the future research agenda is determination of the
20 optimum number of die holes per unit area, their placement and the optimum distance and/or
21 orientation between each of the holes as high pressure may result in deformation of the hole
22 orientation.
23
24

25
26 The above results obtained from the numerical simulation method and RSA approach can
27 provide some reference for the flat die structure design and parameter optimisation. This paper
28 described a simulation-driven design exploration study, which contributes to further research into
29 the utilisation of engineering simulation technology for agricultural machinery/equipment design
30 within the terms of competitive product development activities, in order to survive in today's
31 heavily competitive, high quality, global marketplace.
32
33

34 **Acknowledgements**

35
36 This research study is part-supported financially by The Scientific Research Projects
37 Coordination Unit of Akdeniz University (Turkey) and Lancaster Product Development Unit
38 (LPDU) in Lancaster University (United Kingdom).
39
40
41
42
43
44
45
46
47
48

1
2
3
4
5
6
7
8
9
10
11
12
13
14
15
16
17
18
19
20
21
22
23
24
25
26
27
28
29
30
31
32
33
34
35
36
37
38
39
40
41
42
43
44
45
46
47
48
49
50
51
52
53
54
55
56
57
58
59
60

For Peer Review

References

- 1
2
3
4 ABC Machinery, Pellet Mill Die Decides Your Pellets Production, Available URL:
5 [http://www.bestbiomassmachine.com/solutions/Pellet-Mill-Die-Decides-Your-Pellets-](http://www.bestbiomassmachine.com/solutions/Pellet-Mill-Die-Decides-Your-Pellets-Production.html)
6 [Production.html](http://www.bestbiomassmachine.com/solutions/Pellet-Mill-Die-Decides-Your-Pellets-Production.html), [Last Accessed: 28.08.2017]; 2017a.
- 7
8 ABC Machinery, Pellet Mill Dies, Available URL: [http://www.gemco-energy.com/pellet-mill-](http://www.gemco-energy.com/pellet-mill-dies.html)
9 [dies.html](http://www.gemco-energy.com/pellet-mill-dies.html), [Last Accessed: 28.08.2017]; 2017b.
- 10 Akkurt, M., Machine elements-Power and motion transmission elements (Volume: 3),
11 Birsen Publication, Istanbul-Turkey, 1982. (In Turkish).
- 12 ANSYS Product Documentation, Release Notes: Chapter 5-DesignXplorer, Release 18.1, ANSYS,
13 Inc.; 2017.
- 14
15 Avcil, O.A., The design of spur and helical involute gears with computer support, MSc. Thesis,
16 Yildiz Teknik University; 2006. (In Turkish).
- 17
18 Banuta, M. and Tarquini, I., Fatigue failure of a drive shaft, Eng. Fail. Anal, Vol. 12 (2), p 139-144;
19 2012.
- 20
21 Box, G.E.P. and Draper, N.R., Empirical Model Building and Response Surfaces, Wiley, New
22 York; 1987.
- 23
24 Briggs, J.L., Maier, D.E., Watkins, B.A. and Behnke, K.C., Effect of ingredients and processing
25 parameters on pellet quality. Poultry Science 78: p 1464-1471; 1999.
- 26
27 California Pellet Mill Co. Roskamp Champion. Dies and Die Selection – Die Metallurgy. Available
28 URL: <https://www.cpm.net/downloads/Dies%20and%20Die%20Selection.pdf> [Last Accessed:
29 28.08.2017]; 2015.
- 30
31 Celma, A.R., Cuadros, F., Rodriguez, F.L., Characterization of Pellets from Industrial Tomato
32 Residues. Food and Bioproducts Processing, 90: p 700-706; 2012.
- 33
34 Ciolkosz, D., Hilton, R., Swackhamer, C., Yi, H., Puri, V.M., Swomley, D., Roth, G., Farm-Scale
35 Biomass Pelletizer Performance for Switchgrass Pellet Production, American Society of
36 Agricultural and Biological Engineers, ISSN: 0883-8542; 2013. DOI 10.13031/aea.31.10803.
37 Vol. 31(4): 559-567
- 38
39 Dabnichki, P. and Crocombe A., Finite element modelling of local contact conditions in gear teeth.
40 The Journal of Strain Analysis for Engineering Design, 34 (2), p 129-142; 1999.
- 41
42 Döring, S., Power from Pellets, Springer-Verlag Berlin Heidelberg; 2013. DOI: 10.1007/978-3-642-
43 19962-2_2
- 44
45 Garcia-Maraver, A., Popov, V. And Zamorano, M., A review of European standards for pellet
46 quality. Renewable Energy, 36, 3537-3540; 2011.
- 47
48 Garcia-Maraver, M. Carpio. Biomass pelletization process, in: A. Garcia-Maraver, J.A. Pérez-
49 Jiménez (Eds.), Biomass Pelletization: Standards and Production, WIT Press, Southampton, UK
50 pp. 53–66; 2015.
- 51
52 Holm, J.K., Henriksen, U.B., Hustad, J.E., Sorensen, L.H., Toward an Understanding of Controlling
53 Parameters in Softwood and Hardwood Pellet Production. Energy and Fuel, 20: 2686-2694;
54 2006.
- 55
56 Hu, J., Lei, T., Shen, S., Zhang, Q., Optimal design and evaluation of a ring die granulator for
57 straws, Bioresources 7(1), 489-503; 2011.
- 58
59 Jackson, J., Turner, A., Mark, T., Montross, M., Densification of biomass using a pilot scale flat
60 ring roller pellet mill. Fuel Processing Technology 148: 43–49; 2016.

- 1
2
3
4
5
6
7
8
9
10
11
12
13
14
15
16
17
18
19
20
21
22
23
24
25
26
27
28
29
30
31
32
33
34
35
36
37
38
39
40
41
42
43
44
45
46
47
48
49
50
51
52
53
54
55
56
57
58
59
60
- Mani, S., Tabil, L.G., Sokhansanj, S., An Overview of Compaction of Biomass Grinds. *Powder Handling and Process*, 15: 160-168; 2003.
- Mani, S., Tabil, L.G., Sokhansanj, S., Grinding performance and physical properties of wheat and barley straws, corn stover and switchgrass. *Biomass and Bioenergy*, 27: p 339-352; 2004.
- Milovančević, M., Stefanović-Marinović, J., Anđelković, B., Veg, A., Embedded Condition Monitoring of Power Transmission of A Pellet Mill. *TRANSACTIONS OF FAMENA XXXIV-2* p.71-79; 2010.
- Moon, Y-H., Yang, J., Koo, B-C., An, J-W., Cha, Y-L., Youn, Y-M., Yu, G-D., An, G-H., Park, K-G., Choi, I-H., Analysis of Factors Affecting Miscanthus Pellet Production and Pellet Quality using Response Surface Methodology. *BioResources*, 9(2), 3334-3346; 2014.
- Nilsson, D., Bernesson, S., Hansson, P.A., Pellet Production from Agricultural Raw Materials – A Systems Study. *Biomass and Bioenergy*, 35: 679-689; 2011.
- PelHeat.com, The Beginner's guide to pellet production, Available URL: http://www.pelheat.com/The_Beginners_Guide_To_Making_Pellets.pdf [Last Accessed: 28.08.2017]; 2015.
- Peng, J. H., Bi, H.T., Lim, C. J. and Sokhansanj, S. Study on density, hardness, and moisture uptake of torrefied wood pellets, *Energy Fuels* 27, 967–974; 2013. [dx.doi.org/10.1021/ef301928q](https://doi.org/10.1021/ef301928q)
- Protić, M., Mitić, D., Stefanović, V., Wood Pellets Production Technology Vol 1, No1. 23-26; 2011.
- Puig-Arnabat, M., Shang, L., Sárossy, Z., Ahrenfeldt, J., Henriksen, U. B., From a single pellet press to a bench scale pellet mill — Pelletizing six different biomass feedstocks, *Fuel Processing Technology* 142, p 27–33; 2016.
- Salas-Bringas, C., Filbakk, T., Skjevraak, G., Lekang, O.I., Hoibo, O., Schuller, R.B., Compression rheology and physical quality of wood pellets pre-handled with four different conditions. *Annual Transactions of the Nordic Rheology Society*. Vol 18. p 87-93; 2010.
- Standard EN 16127. Solid biofuels – Determination of length and diameter for pellets and cylindrical briquettes.
- Stelte, W., Holm, J.K., Sanadi, A.R., Barsberg, S., Ahrenfeldt, J. and Henriksen, U.B., Fuel pellets from biomass: The importance of the pelletizing pressure and its dependency on the processing conditions, *Fuel* Volume 90, Issue 11, November 2011, Pages 3285–3290
- Theerarattanoon, K., Xu, F., Wilson, J., Ballard, R., McKinney, L., Staggenborg, S., Vadlani, P., Pei, Z.J., Wang, D., Physical Properties of Pellets Made from Sorghum Stalk, Corn Stover, Wheat Straw, and Big Bluestem. *Industrial Crops and Products*, 33(2): p 325-332; 2011.
- Werther, J., Sanger, M., Hartge, E.U., Ogada, T., Siagi, Z., Combustion of Agricultural Residues. *Progress in Energy and Combustion Science*, 26: p 1-27; 2000.
- Yilmaz, H., “A Research on the pelleting of various agricultural residues and determination of pellet physical properties”, MSc. Thesis, Akdeniz University; 2014. (In Turkish).
- Zamorano, M., Popov, V., Rodríguez, M.L., García-Maraver, A., A comparative study of quality properties of pelletized agricultural and forestry lopping residues. *Renewable Energy*, 36: 3133-3140; 2011.

1
2
3
4
5
6
7
8
9
10
11
12
13
14
15
16
17
18
19
20
21
22
23
24
25
26
27
28
29
30
31
32
33
34
35
36
37
38
39
40
41
42
43
44
45
46
47
48
49
50
51
52
53
54
55
56
57
58
59
60

FIGURE CAPTIONS

Figure 1. Biomass pelletizing process

Figure 2. Some failure samples seen on the die element

Figure 3. FEA simulation setup, FE model and simulation print outs

Figure 4. Comparison of the predictions from solved specific design points and predictions from response surface data

Figure 5. Response surface charts

For Peer Review

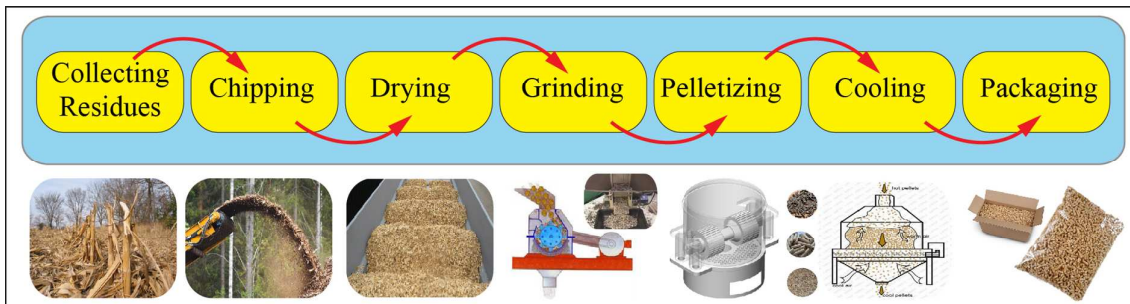


Figure 1. Biomass pelletizing process

For Peer Review

1
2
3
4
5
6
7
8
9
10
11
12
13
14
15
16
17
18
19
20
21
22
23
24
25
26
27
28
29
30
31
32
33
34
35
36
37
38
39
40
41
42
43
44
45
46
47
48
49
50
51
52
53
54
55
56
57
58
59
60

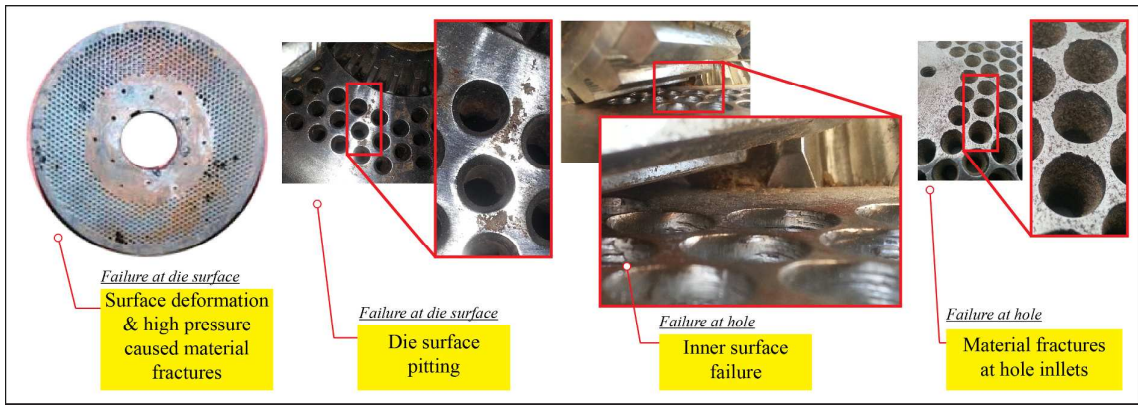


Figure 2. Some failure samples seen on the die element

For Peer Review

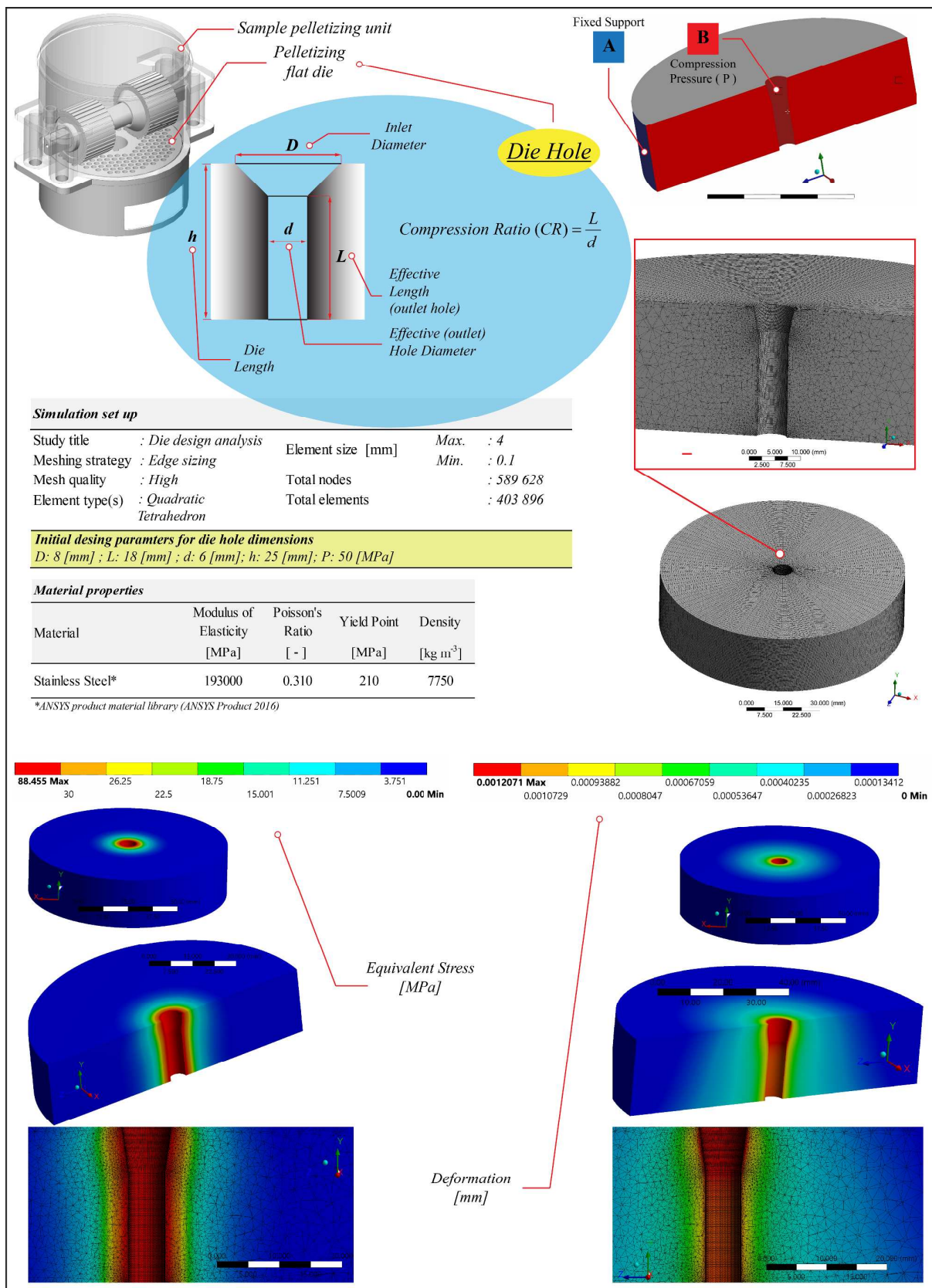


Figure 3. FEA simulation setup, FE model and simulation print outs

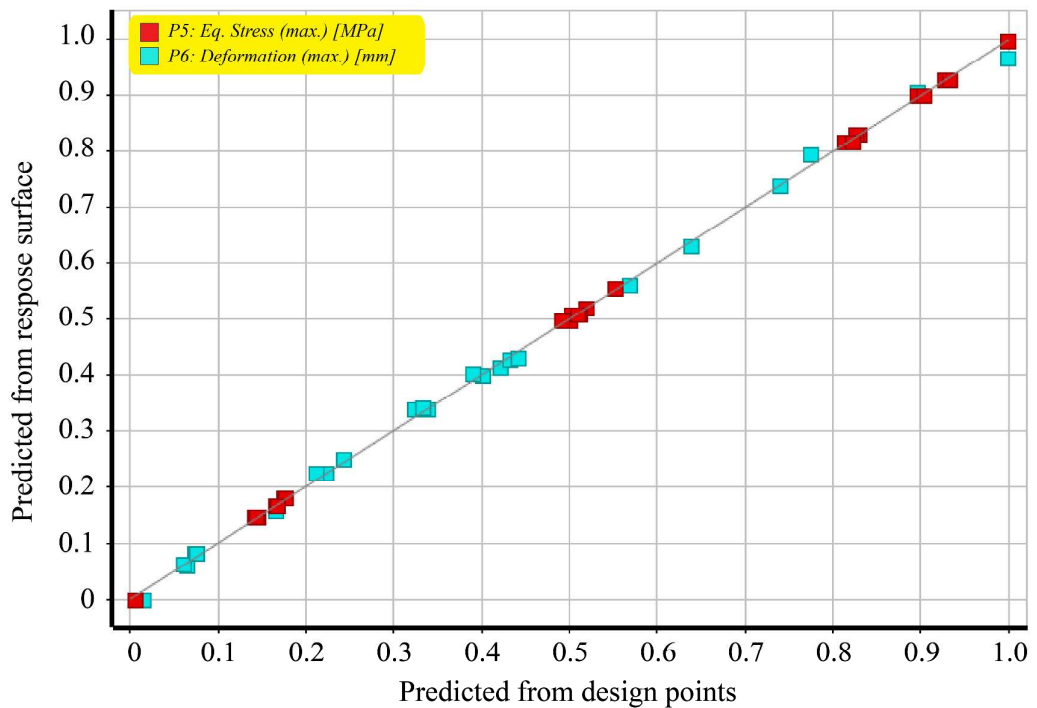


Figure 4. Comparison of the predictions from solved specific design points and predictions from response surface data

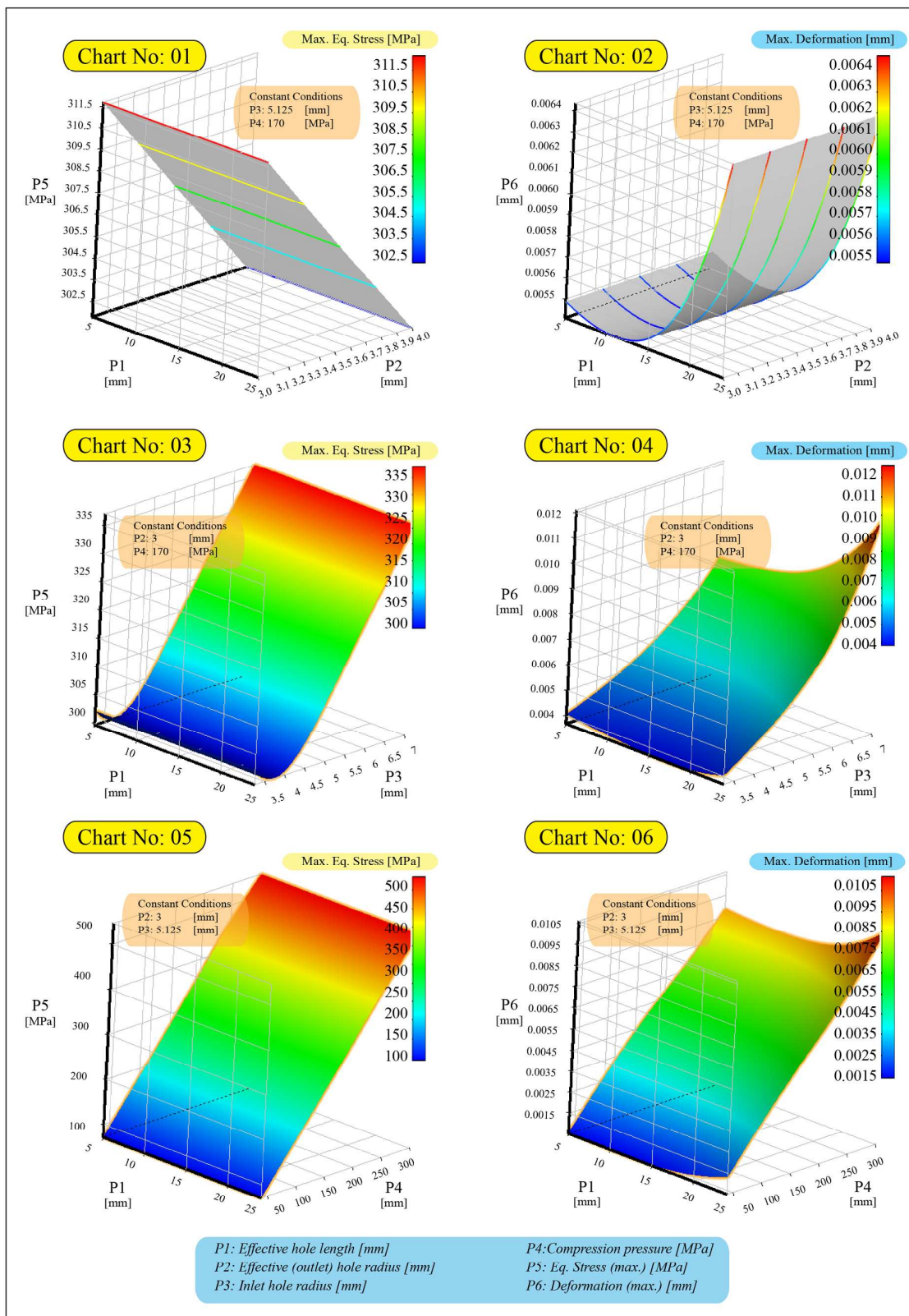


Figure 5. Response surface charts

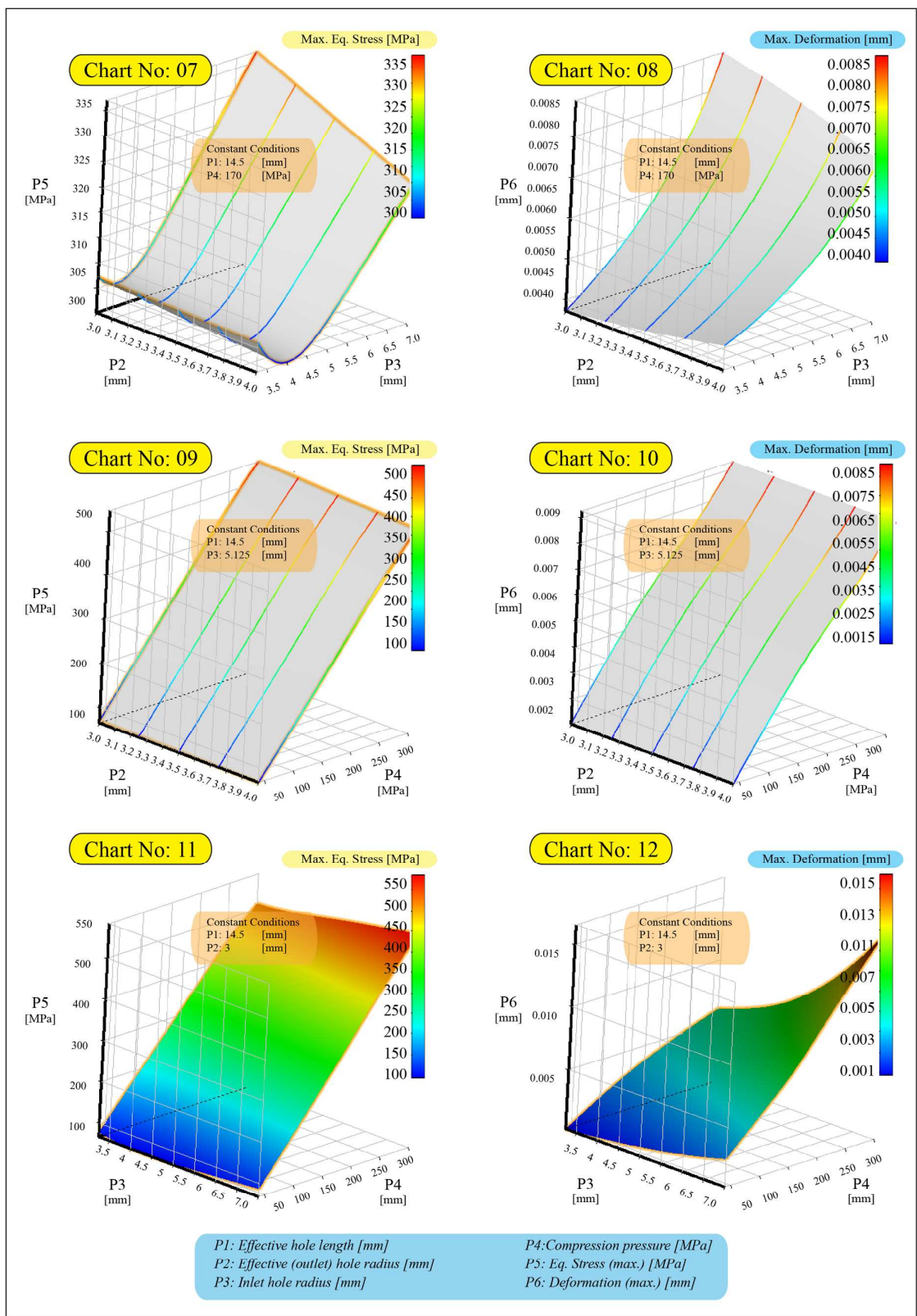


Figure 5. Response surface charts (Continued)

TABLE CAPTION

Table 1. Design parameters and response parameters

Table 2. Estimation model parameters by RSM charts

For Peer Review

Table 2. Estimation model parameters by RSM charts

Parameter	Estimate	Std.Error	t Value	Pr > t	Partial F-Ratio Test
B_0	344.902929	0.015008	22981.9	0.0001	3.841E8 (0.0001)
P2	-11.680094	0.008481	-1377.3	0.0001	
P1	-1.39E-13	0.000253	0	1	
P1*P1	0	0.000004328	0	1	23162.4 (0.0001)
P2*P2	0.259038	0.001204	215.23	0.0001	
P1*P2	0	0.000062361	0	1	0.00 (0.9756)
P5 R ² =1.000 F-value = 1.536E8 (total regression)					Prob. =0.0001
Parameter	Estimate	Std.Error	t Value	Pr > t	Partial F-Ratio Test
B_0	0.006029	0.000432	13.95	0.0001	2115.37 (0.0001)
P3	0	0.000244	0	1	
P2	-0.000122	0.000007281	-16.78	0.0001	
P2*P2	0.000005639	0.000000125	45.22	0.0001	1022.50 (0.0001)
P3*P3	0	0.000034672	0	1	
P2*P3	0	0.000001797	0	1	0.00 (1.0000)
P6 R ² =0.981 F-value = 1255.14 (total regression)					Prob. =0.0001
Parameter	Estimate	Std.Error	t Value	Pr > t	Partial F-Ratio Test
B_0	310.700721	1.435659	216.42	0.0001	24427.5 (0.0001)
P3	-10.378619	0.513509	-20.21	0.0001	
P1	0	0.070631	0	1	
P1*P1	0	0.001885	0	1	907.49 (0.0001)
P3*P3	2.061708	0.048394	42.6	0.0001	
P1*P3	0	0.008523	0	1	0.00 (1.0000)
P5 R ² =0.988 F-value = 10134.0 (total regression)					Prob. =0.0001
Parameter	Estimate	Std.Error	t Value	Pr > t	Partial F-Ratio Test
B_0	0.009372	0.000171	54.91	0.0001	29753.4 (0.0001)
P3	-0.002032	0.000061045	-33.29	0.0001	
P1	-0.000377	0.000008396	-44.95	0.0001	
P1*P1	0.000006957	0.000000224	31.04	0.0001	1575.43 (0.0001)
P3*P3	0.000269	0.000005753	46.77	0.0001	
P1*P3	0.000045246	0.000001013	44.66	0.0001	1994.47 (0.0001)
P6 R ² =0.991 F-value = 12930.4 (total regression)					Prob. =0.0001
Parameter	Estimate	Std.Error	t Value	Pr > t	Partial F-Ratio Test
B_0	-7.421723	0.750629	-9.89	0.0001	1825626 (0.0001)
P4	1.917512	0.005437	352.7	0.0001	
P1	0	0.082208	0	1	
P1*P1	0	0.002613	0	1	77.16 (0.0001)
P4*P4	-0.000173	0.000013954	-12.42	0.0001	
P1*P4	0	0.00017	0	1	0.00 (1.0000)
P5 R ² =0.999 F-value = 730281 (total regression)					Prob. =0.0001
Parameter	Estimate	Std.Error	t Value	Pr > t	Partial F-Ratio Test
B_0	0.000707	0.000041786	16.93	0.0001	171394 (0.0001)
P4	0.000033796	0.000000303	111.66	0.0001	
P1	-0.000169	0.000004576	-37.04	0.0001	
P1*P1	0.000006486	0.000000145	44.59	0.0001	1154.57 (0.0001)
P4*P4	-1.39E-08	7.77E-10	-17.91	0.0001	
P1*P4	0.000000169	9.48E-09	17.79	0.0001	316.39 (0.0001)
P6 R ² =0.998 F-value = 69082.5 (total regression)					Prob. =0.0001

Table 2. Estimation model parameters by RSM charts (continued)

Parameter	Estimate	Std.Error	t Value	Pr > t	Partial F-Ratio Test
<i>B</i> ₀	295.220163	16.422697	17.98	0.0001	3375.93 (0.0001)
P3	-3.188724	1.637682	-1.95	0.0539	
P2	7.059154	8.835916	0.8	0.4259	
P2*P2	0.237022	1.238517	0.19	0.8486	215.29 (0.0001)
P3*P3	2.372642	0.114346	20.75	0.0001	
P2*P3	-3.462742	0.32515	-10.65	0.0001	113.42 (0.0001)
P5 R ² =0.9840 F-value = 1459.17 (total regression)					Prob. =0.0001
Parameter	Estimate	Std.Error	t Value	Pr > t	Partial F-Ratio Test
<i>B</i> ₀	-0.002545	0.000701	-3.63	0.0004	25053.6 (0.0001)
P3	0.000585	0.000069902	8.36	0.0001	
P2	0.002181	0.000377	5.78	0.0001	
P2*P2	-0.000007876	0.000052864	-0.15	0.8818	816.75 (0.0001)
P3*P3	0.000197	0.000004881	40.42	0.0001	
P2*P3	-0.000431	0.000013879	-31.06	0.0001	964.46 (1.0000)
P6 R ² =0.998 F-value = 10541.0 (total regression)					Prob. =0.0001
Parameter	Estimate	Std.Error	t Value	Pr > t	Partial F-Ratio Test
<i>B</i> ₀	0.296189	20.592507	0.01	0.9885	339435 (0.0001)
P4	2.079241	0.024663	84.3	0.0001	
P2	-3.616252	11.697203	-0.31	0.7577	
P2*P2	0.269992	1.662537	0.16	0.8713	20.69 (0.0001)
P4*P4	-0.000205	0.00003193	-6.43	0.0001	
P2*P4	-0.05034	0.006295	-8	0.0001	63.94 (0.0001)
P5 R ² =0.999 F-value = 135795 (total regression)					Prob. =0.0001
Parameter	Estimate	Std.Error	t Value	Pr > t	Partial F-Ratio Test
<i>B</i> ₀	-0.000345	0.000703	-0.49	0.6248	82110.9 (0.0001)
P4	0.00003684	0.000000842	43.76	0.0001	
P2	0	0.000399	0	1	
P2*P2	0	0.000056755	0	1	133.24 (0.0001)
P4*P4	-1.78E-08	1.09E-09	-16.32	0.0001	
P2*P4	0	0.000000215	0	1	0.00 (1.0000)
P6 R ² =0.999 F-value = 32897.7 (total regression)					Prob. =0.0001
Parameter	Estimate	Std.Error	t Value	Pr > t	Partial F-Ratio Test
<i>B</i> ₀	42.871929	2.601062	16.48	0.0001	971243 (0.0001)
P4	1.586728	0.008954	177.2	0.0001	
P3	-19.589155	0.9641	-20.32	0.0001	
P3*P3	1.96876	0.091566	21.5	0.0001	282.24 (0.0001)
P4*P4	-0.000193	0.000019048	-10.11	0.0001	
P3*P4	0.062848	0.001178	53.33	0.0001	2844.48 (0.0001)
P5 R ² =0.999 F-value = 389179 (total regression)					Prob. =0.0001
Parameter	Estimate	Std.Error	t Value	Pr > t	Partial F-Ratio Test
<i>B</i> ₀	0.007068	0.000261	27.1	0.0001	44747.8 (0.0001)
P4	-0.000006792	0.000000898	-7.56	0.0001	
P3	-0.003032	0.000096666	-31.36	0.0001	
P3*P3	0.000299	0.000009181	32.6	0.0001	538.64 (0.0001)
P4*P4	-7.26E-09	1.91E-09	-3.8	0.0002	
P3*P4	0.000008396	0.000000118	71.06	0.0001	5049.95 (0.0001)
P6 R ² =0.994 F-value = 19124.6 (total regression)					Prob. =0.0001